MAGNETIC BEHAVIOR AND MAGNETO-IMPEDANCE EFFECT IN CoFeBSi RIBBONS

COMPORTAMIENTO MAGNÉTICO Y EFECTO DE MAGNETO-IMPEDANCIA EN CINTAS DE CoFeBSi

Abilo A. Velásquez[†‡*], Mónica Gómez-Hermida[§], Andrés Rosales-Rivera[†x]

[†] Laboratorio de Magnetismo y Materiales Avanzados, Facultad de Ciencias Exactas y Naturales, Universidad Nacional de Colombia, Sede Manizales, Manizales, Colombia
[‡] Departamento de Ingeniería Eléctrica, Electrónica y Computación, Facultad de Ingeniería y Arquitectura, Universidad Nacional de Colombia, Sede Manizales, Manizales, Colombia.
[§] Departamento de Ciencias Básicas, Universidad Católica de Pereira, Pereira, Colombia y Facultad de Minas, Universidad Nacional de Colombia, Sede Medellín, Medellín, Colombia.

(Recibido: 09/2012. Aceptado: 12/2012)

Abstract

In this paper we present *dc* magnetization, *ac* susceptibility and impedance measurements on amorphous alloy ribbons $Co_{80-x}Fe_xB_{10}Si_{10}$ with x = 0, 6, 8 and 10 at.%. They indicate that at room temperature these samples have good soft magnetic behavior including the giant magneto-impedance effect. The real part of the *ac* susceptibility $\chi' ac$ reveals an irreversibility field, H_{irr}, which corresponds to the transverse anisotropy field, H_k, at which the magneto-impedance ratio reaches its maximum value.
PACS: 75; 75.50.-y; 75.50.Bb

Keywords: Soft ferromagnetic alloys, magnetic behavior, giant magneto-impedance effect.

Resumen

En este trabajo, presentamos medidas de magnetización *dc*, susceptibilidad *ac* e impedancia en cintas de la aleación

* aavelasquezs@unal.edu.co
x arosalesr@unal.edu.co

amorfa $Co_{80-x}Fe_xB_{10}Si_{10}$ con x = 0, 6, 8 y 10 %.at. Esas medidas indican que a temperatura ambiente esas muestras tienen buen comportamiento magnético blando incluyendo el efecto de magneto-impedancia gigante. La parte real de la susceptibilidad ac, $\chi' ac$, revela un campo de irreversibilidad, H_{irr}, el cual corresponde al campo de anisotropía transversal, H_k, donde la razón de la magneto-impedancia alcanza su valor máximo.

Palabras clave: Aleaciones magnéticas blandas, comportamiento magnético, efecto de magneto-impedancia gigante.

Introduction

Cobalt-based amorphous magnetic alloy ribbons have been integrated in high-frequency transformer and magnetic recording heads since 1980 [1] due to their interesting physical properties such as high magnetic permeability and low magnetostriction. Interest in this alloy system is also associated with the presence of giant magneto-impedance (GMI) effect in soft magnetic materials, as detected at the beginning of the 1990s [2–5]. The GMI effect consists of large variations in impedance of a soft ferromagnetic conductor upon the application of a small *dc* magnetic field when an *ac* current flows through it. The GMI ratio with H is defined as $\Delta Z/Z\ (\%) = 100[Z(H)\text{-}Z\ (H_{max})]/Z(H_{max})$, where $Z(H)$ and $Z(H_{max})$ are the impedance measured at any and maximum applied magnetic field H_{max} ($H_{max} \approx 80$ Oe in our case) at which the soft magnets are practically saturated. In general, the GMI effect depends on the *dc* applied magnetic field, the working frequency of the *ac* current, the domain structure of the material, and the magnetic anisotropies that are present in the material. The magnetic penetration depth, $\delta = c(4\pi^2 f\sigma\mu)^{-1/2}$, where f denotes the frequency of the current along the sample, σ the electrical conductivity, and μ the magnetic permeability (transversal, in case of the ribbons), is also relevant to determine the magneto-impedance (MI) response [5]. Depending on the frequency of the *ac* current, the experimentally observed GMI curves usually exhibit two types of behaviors, specifically single-peak (SP),

and two-peaks (TP). These behaviors depend upon the relative contributions of domain-wall motion and magnetization rotation processes to the magnetic permeability, $\mu = \mu_{wall} + \mu_{rot}$ [5–9]. At low frequencies (on the order of $f \leq 2$ MHz), the main event is the SP behavior and the magnetoimpedance is due to domain-wall motion [5]. At higher frequencies (in the range $2 \leq f \leq 20$ MHz), the important event is the TP behavior and in this case the magnetization rotation process is dominant [10] since domain-wall motion is absent by the eddy currents damping. The damping of the domain wall has been confirmed by Kerr effect domain inspection [11].

The *ac* magnetic susceptibility, on the other hand, in which a small *ac* magnetic field is applied to a sample and the resulting *ac* moment is measured, is a basic tool for characterizing many materials. Due to that the induced moment in the sample depends upon the time, *ac* magnetic susceptibility measurements provide information on magnetization dynamics which plays an important role in the interpretation of GMI effect. Gonçalves et. al. [12] claim from *ac* susceptibility studies, that small samples of soft ferromagnetic materials become magnetically harder because the magnetic domain configurations are strongly influenced by the demagnetizing field.

In this paper a systematic study of the *dc* magnetization, *ac* susceptibility and magneto-impedance effect, in amorphous alloy ribbons $Co_{80-x}Fe_xB_{10}Si_{10}$ with $x = 0$, 6, 8 and 10 (here x is referred to Fe concentration in atomic percentage, at.%), is presented. CoFe-based amorphous magnetic alloy ribbons have interesting physical properties [13, 14], such as low magnetostriction, which make them promissory materials in order to obtain high magneto-impedance response. Although there are several reports [5] of their good soft magnetic properties, the relation between *ac* susceptibility and magneto-impedance effect in these alloys has been scarcely studied. The main purpose of this paper is to gain an understanding on the *ac* magnetic susceptibility and magneto-impedance of alloy system $Co_{80-x}Fe_xB_{10}Si_{10}$ where Co was gradually replaced by Fe.

Experimental Details

The experiments were performed on samples of as-cast ribbons $Co_{80-x}Fe_xB_{10}Si_{10}$ with $x = 0$, 6, 8 and 10, prepared by the melt spinning technique. The amorphous state of each of the samples was verified by X-ray diffraction (XRD) using a Rigaku Miniflex II diffractometer with CuKα radiation ($\lambda = 1.5405$ Å) in the $20^o \leq 2\theta \leq 100^o$ range at steps of 0.02 s^{-1}. The *dc* magnetic field (H) dependence of the magnetization, $M(H)$, of the samples under study was measured, from -1 to 1 KOe at room temperature, with a home-made Foner-type vibrating sample magnetometer. H was applied parallel to the longitudinal direction of the samples. Data were obtained for consecutive H-steps, stabilizing H before each reading with a precision of ±20 Oe. The *ac* susceptibility of the samples was measured for *dc* magnetic field (H) applied in the range -80 to 80 Oe at room temperature, using the standard *ac* inductance method. The frequency of the *ac* modulating field was applied in the range 10 to 10^4 Hz, while its amplitude was maintained at $H_{ac} \sim 1$ Oe. Both H and H_{ac} were applied along the longitudinal direction of the samples. The impedance in the samples was measured for *dc* magnetic field (H) applied in the range -80 to 80 Oe at room temperature, via the so-called four-probe technique. H was applied parallel to the *ac* driving current along the longitudinal direction of the samples and was swept at a step of approximately 1 Oe. The frequency of the *ac* driving current was applied in the range 0.5 to 10 MHz, while its amplitude was kept at 1 mA (rms value).

Results and Discussion

The $M(H)$-cycle at room temperature for samples $x = 6$, 8 and 10 is presented in Fig.1. The curves in Fig. 1 are typical of a soft magnetic material, i,e. the hysteresis loop is closed and narrow. Furthermore, these loops have low coercivity and the inclination of the initial magnetization curve (called initial *dc* susceptibility, χ_i) is very high. Note that χ_i increases with increasing x concentration. It is known [15] that for soft magnetic

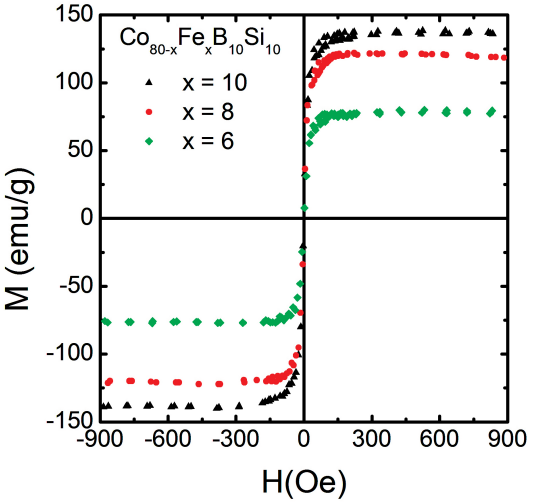

FIGURE 1. *M vs. H measured on* $Co_{80-x}Fe_xB_{10}Si_{10}$ *with* $x = 6$, *8 and 10 at room temperature.*

materials with high permeability, the initial magnetic permeability is roughly equal to the initial *dc* susceptibility ($\mu_i \approx \chi_i$) which is given by

$$\chi_i = (\partial M/\partial H)|_{H\to 0} = (\mu_o M_s^2/cE_A) \qquad (1)$$

where E_A represents several types of anisotropy energy including the magnetoelastic energy. It can be noted by inspection of data in Fig. 1 that the initial magnetic permeability increases with increasing x values. This behavior is compatible with the equation (1) and supported by the Fig. 2, where is plotted the χ_i vs H curve for samples $x = 6$, 8 and 10. The χ_i vs. H curve (not shown here) for the sample $x = 0$ lies below those ones corresponding to the samples $x = 6$, 8 and 10. This permeability behavior indicates that the anisotropy energy decreases with increasing x concentration.
It has been proposed [13] that for amorphous and nanocrystalline alloys, the permeability will have the dependence on the grain size D as μ $1/D^6$. This relation has been confirmed by some permeability experiments [16] for grains smaller than 40nm. However, a detailed and quantitative study on the grain size dependence of the permeability is beyond the scope of this work. In addition, the χ_i vs. H curve quickly decreases with increasing H, which reflects magnetization processes ascribed to domain wall motion

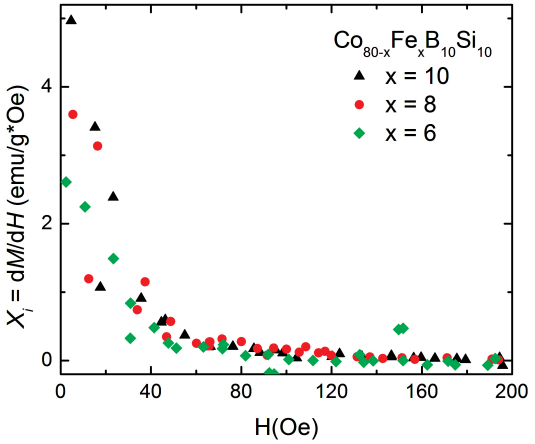

FIGURE 2. *Field dependence of* $\chi_i = dM/dH$ *for* $Co_{70}Fe_{10}B_{10}Si_{10}$ *at room temperature.*

[5, 17]. Another feature evidenced in Fig. 1 is that the saturation magnetization Ms increases from 80 to 137 emu/g with increasing x values. This result may be due to the fact that Fe-based intermetallic alloys do not have their 3d shells fully filled. The moment associated to the atoms of Fe can be increased in agreement with Slater-Pauling curve by increasing the number of electrons in the 3d shell. This can be achieved in samples of CoFe-based alloys since these alloys can host one electron additional in the 3d shell as compared with the Fe-based alloys.

The *dc* magnetic field dependence of the *dc* susceptibility, χ_{dc} (H) $= M/H$, at room temperature, for samples $x = 6$, 8 and 10, is presented in Fig. 3. Note that $\chi_{dc}(H)$ shows a peak around $H = 0$, whose amplitude increases with increasing x values. Furthermore, the $\chi_{dc}(H)$-curve for the sample with $x = 10$ decreases more rapidly with increasing field than that one for the samples with $x = 6$ and 8. These features indicate that the sample with $x = 10$ is the softest magnetically.

The *dc* magnetic field dependence of the real part of the *ac* susceptibility, $\chi' ac$, at room temperature, for sample $x = 0$ for frequencies in the range $40 \leq \mathrm{f} \leq 9000$ Hz, is illustrated in Figs. 4, 5 and 6.

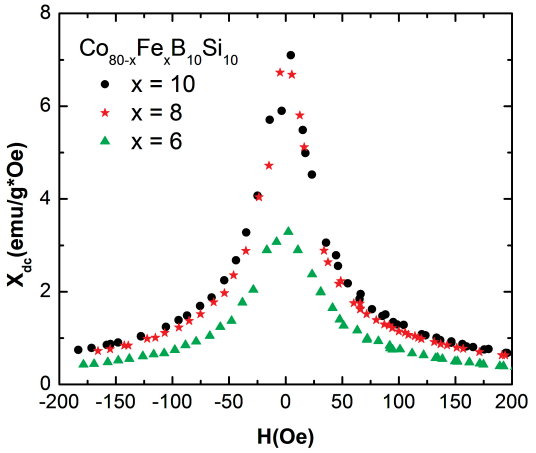

FIGURE 3. *Field dependence of the dc susceptibility, $\chi_{dc} = M/H$ for $Co_{80-x}Fe_xB_{10}Si_{10}$ with $x = 6$, 8 and 10 at room temperature.*

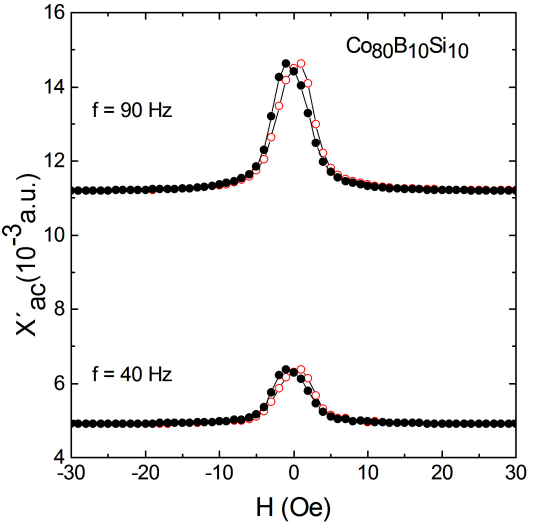

FIGURE 4. *$\chi'ac$ vs. H measured on $Co_{80}B_{10}Si_{10}$ at room temperature using f = 40 and 90 Hz. Filled symbols are field increasing data and open symbols are field decreasing data.*

As shown in Fig. 5 for f = 400 and 700 Hz, the initial $\chi'ac$ curve shows a monotonous decrease from $H = 0$. A very similar decrease was also observed for the frequencies $f = 0.04$, 0.09, 4, and 6 KHz (not shown here). This behavior is a result of magnetization processes attributed to domain wall motion [5, 17] and is consistent

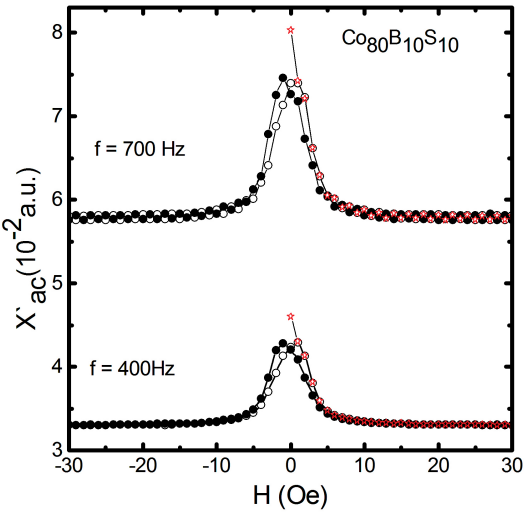

FIGURE 5. *$\chi'ac$ vs.H measured on $Co_{80}B_{10}Si_{10}$ at room temperature using f = 400 and 700 Hz. Filled symbols are field increasing data and open symbols are field decreasing data. The red symbol corresponds to the initial $\chi'ac$ curve.*

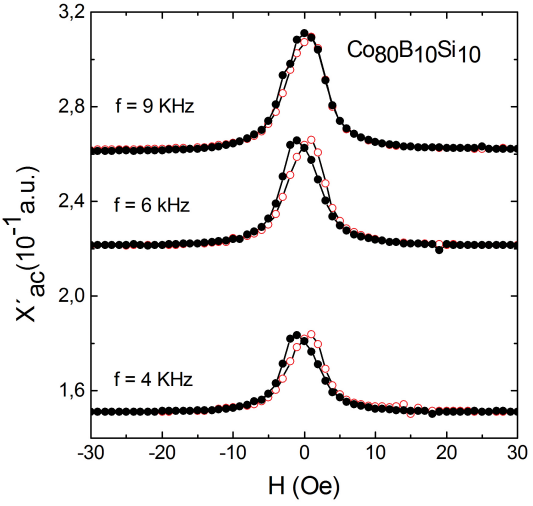

FIGURE 6. *$\chi'ac$ vs. H measured on $Co_{80}B_{10}Si_{10}$ at room temperature using f = 4, 6 and 9 KHz. Filled symbols are field increasing data and open symbols are field decreasing data.*

with the field dependence of the initial *dc* susceptibility χ_i discussed above (see Fig. 2). Another interesting feature illustrated in the Figs. 4, 5, and 6 is the appearance both of a hysteretic peak at

$H = \pm H_o \neq 0$ and an *ac* susceptibility irreversible behavior. The *ac* susceptibility irreversible behavior is limited to the vicinity of H_o and it is possible to define an irreversibility field H_{irr} as that one above which irreversible behavior of *ac* susceptibility hysteresis loops disappears. The irreversibility field, H_{irr}, is correlated with the field at which appears the GMI effect's TP behavior as will be analyzed in more detail later on.

A slightly different behavior is observed at sample $x = 10$. In this case, $\chi' ac$-curve exhibits very small hysteresis and the peak at close vicinity of $H = 0$ becomes excessively broad, as shown in Fig. 7, where is plotted $\chi' ac(H)$ for the sample with $x = 10$ at frequencies $f = 40$ and 90 Hz. On the other hand, at low-frequency region an *ac* measurement is very similar to a *dc* measurement [15]. In our case, this is easily seen by comparing the Figs. 2 and 7.

The *dc* magnetic field dependence of the GMI ratio for samples $x =$ 0, 6, and 10 at room temperature, for $0.5 \leq f < 10$ MHz is shown in Figs. 7, 8 and 9, respectively. All samples exhibit GMI effect as it is expected to occur in materials with very soft magnetic properties and low magnetostriction [18]. In the frequency range used in our experiments ($0.5 \leq f < 10$ MHz), the skin effect is very strong because both, domain wall motion and magnetization rotation contribute to the effective transversal permeability. Consequently, it is expected to observe the SP and TP behaviors. In fact, these behaviors were observed in the samples here studied but they occur in different frequency regions that depend upon the sample under study. In this respect the following comments should be underlined: (1) it is observed a relatively large (on the order of 20%) magneto-impedance in the three samples, (2) in the sample with x $= 0$ (Fig. 8) the SP behavior is not observed, and (3) in contrast to the symmetric TP behavior observed in the samples with $x = 6$ and 10, the GMI curve in the sample with $x = 0$ exhibits an asymmetric TP behavior characterized by an increase of one of the peaks while the other one is reduced. Looking at the magneto-impedance effect in detail for the sample with $x = 0$ we can observe that the TP behavior that occurs at $H = \pm H_k \neq 0$ coincides quite well with the *dc* irreversibility field, $\pm H_{irr}$, of the $\chi' ac$ curve, as evidenced by Figs. 4, 5, 6, and 8. This concordance clearly supports the

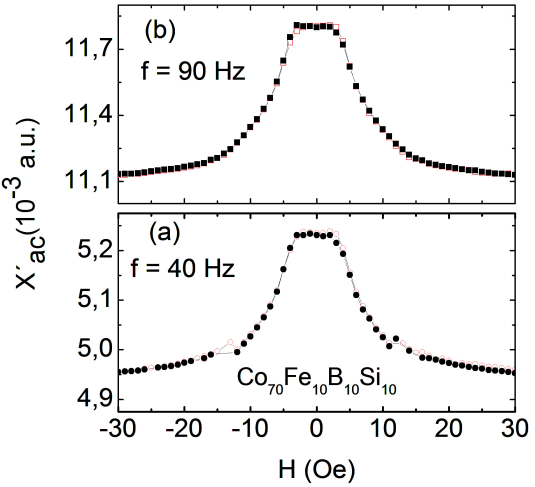

FIGURE 7. *$\chi'ac$ vs.H measured on $Co_{70}Fe_{10}B_{10}Si_{10}$ at room temperature using $f = 40$ and 90 Hz. Filled symbols are field increasing data and open symbols are field decreasing data.*

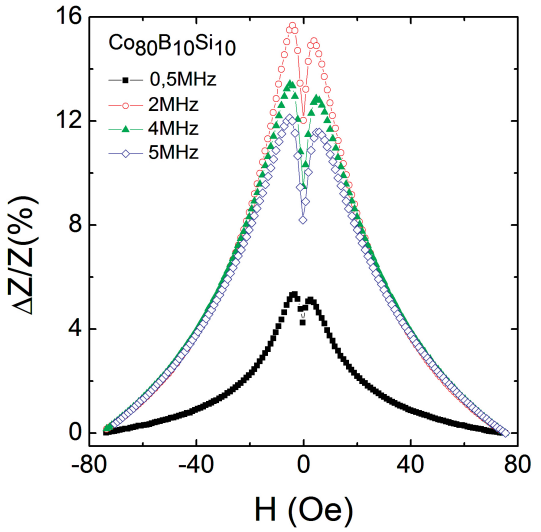

FIGURE 8. *GMI ratio vs. H measured on $Co_{80}B_{10}Si_{10}$ at room temperature for different frequencies $f = 0.5$, 2, 4 and 5 MHz.*

identification of the field at which the magneto-impedance ratio reaches its maximum value as the field at which the irreversible magnetization process is completed. In this context, H_k is the transverse magnetic anisotropy field. This transversal anisotropy is

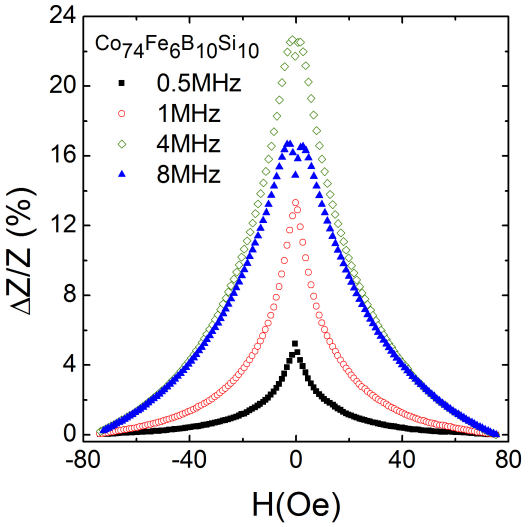

FIGURE 9. *GMI ratio vs. H measured on $Co_{74}Fe_6B_{10}Si_{10}$ at room temperature for different frequencies f = 0.5, 1, 4 and 8 MHz.*

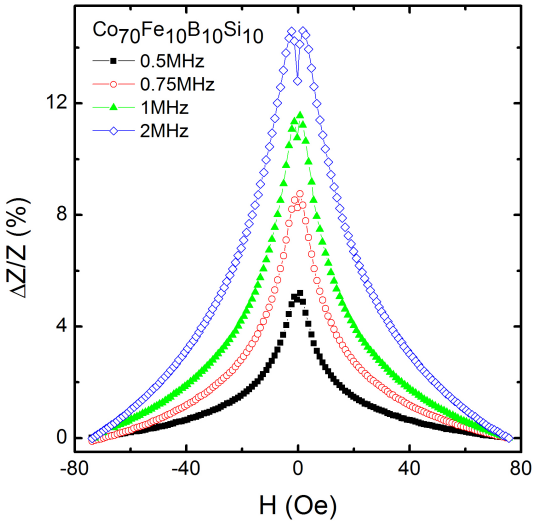

FIGURE 10. *GMI ratio vs. H measured on $Co_{70}Fe_{10}B_{10}Si_{10}$ at room temperature for different frequencies f = 0.5, 0.75, 1 and 2 MHz.*

due to the combined effect of the negative magnetostriction and the internal stress frozen during the fabrication process of the material [5, 18]. In the case of the sample with $x = 10$, H_{irr} is slightly higher than H_k, as evidenced by Figs. 7 and 10, and H_k shifts

to higher fields, with increasing f. This shifting is attributed to the increasing average magnetoelastic anisotropy involved in the skin-effect penetration depth [5].

Conclusion

We have made a study of the *dc* magnetization, *ac* susceptibility and magneto-impedance in the alloy system $Co_{80-x}Fe_xB_{10}Si_{10}$ with $x = 0$, 6, 8 and 10. All samples exhibit soft magnetic behavior including the giant magneto-impedance effect. This behavior is consistent with the field dependences of the *dc* magnetization and *ac* susceptibility. The real part of the *ac* susceptibility, $\chi' ac$, reveals an irreversibility field, H_{irr}, which corresponds to the transverse anisotropy field, H_k, at which the magneto-impedance ratio reaches its maximum value.

Acknowledgments

The authors acknowledge Professor D. Muraca for fruitful discussions and collaborations. The authors, A.A. Velásquez and M. Gómez, also acknowledge the support of Colciencias (Colombian agency). Work at the Universidad Nacional de Colombia, Branch of Manizales, is supported by the Research Office (DIMA). The samples were prepared at Laboratorio de Sólidos Amorfos, Facultad de Ingeniería, Universidad de Buenos Aires, Argentina.

References

[1] Y. Makino, in *Physics and Engineering Applications of Magnetism*, Springer Series in Solid-State Sciences, Vol. 92, edited by Y. Ishikawa and N. Miura (Springer Berlin Heidelberg, 1991) pp. 195–210.

[2] V. Makhotkin, B. Shurukhin, V. Lopatin, P. Marchukov, and Y. Levin, Sens. Actuators, A **27**, 759 (1991).

[3] F. L. A. Machado, B. L. da Silva, and E. Montarroyos, J. Appl. Phys. **73**, 6387 (1993).

[4] K. Mandal and S. K. Ghatak, Phys. Rev. B **47**, 14233 (1993).

[5] K. Buschow, *Handbook of Magnetic Materials*, Handbook of Magnetic Materials No. v. 15 (Elsevier Science, 2003) pp. 497–563.

[6] D. Atkinson and P. T. Squire, J. Appl. Phys. **83**, 6569 (1998).

[7] K. R. Pirota, L. Kraus, M. Knobel, P. G. Pagliuso, and C. Rettori, Phys. Rev. B **60**, 6685 (1999).

[8] L. Panina, K. Mohri, T. Uchiyama, M. Noda, and K. Bushida, IEEE Trans. Magn. **31**, 1249 (1995).

[9] M. Tejedor, B. Hernando, M. Sánchez, M. Vázquez, and M. Knobel, J. Magn. Magn. Mater. **152**, 191 (1996).

[10] K. Byon, S. Yu, J. Kim, and C. Kim, IEEE Trans. Magn. **37**, 3086 (2001).

[11] L. Melo and A. Santos, in *Magnetism, Magnetic Materials and Their Applications*, Materials Science Forum, Vol. 302-3, edited by Missell, FP (1999) pp. 219–223.

[12] L. Gonçalves, J. Soares, F. Machado, and W. de Azevedo, Physica B: Condensed Matter **384**, 152 (2006).

[13] G. Herzer, Acta Materialia **61**, 718 (2013).

[14] M. Coisson, P. Tiberto, F. Vinai, P. Tyagi, S. Modak, and S. Kane, J. Magn. Magn. Mater. **320**, 510 (2008).

[15] R. Grossinger, H. Sassik, D. Holzer, and N. Pillmayr, *Magnetic characterization of soft magnetic materials: experiments and analysis*, Vol. 254-255 (2003) pp. 7 – 13.

[16] G. Herzer, J. Magn. Magn. Mater. **157-158**, 133 (1996).

[17] L. Panina and K. Mohri, *Magneto-impedance in multilayer films*, Vol. 81 (2000) pp. 71 – 77.

[18] M. Vazquez, J. Sinnecker, and G. Kurlyandskaya, in *Magnetism, Magnetic Materials and their Applications*, Materials Science Forum, Vol. 302-3, edited by Missell, FP (1999) pp. 209–218.